Theor Chim Acta (1994) 89: 363–374

Theoretica Chimica Acta

© Springer-Verlag 1994

The S-matrix version of the Hulthén–Kohn variational principle for quantum scattering: Finite element calculations for state-to-state reaction probabilities*

Ralph Jaquet, Julia Gribkova
Theoretical Chemistry, University Siegen, P.O. Box 101240, D-57068 Siegen, Germany

Received March 24, 1994/Final revision received June 9, 1994/Accepted August 15, 1994

Summary. The finite element (FE) method can be applied to solve the reactive scattering problem of the A + BC → AB + C type. We are using the S-matrix version of the Hulthén–Kohn variational principle for the two-dimensional collinear problem. The asymptotic wavefunction is described by analytical functions and the interaction part by FE functions.

Two approaches are used and compared to each other: 1) FE functions are employed as the basis functions for the interior part of the potential; 2) the FE method is used in order to calculate eigenfunctions for the interior region of the potential and then these eigenfunctions are used as a new basis. In the second case two ways of choosing grid points are applied. First a grid is built that covers both reaction channels, secondly we considered the two reactions channels separately and two basis sets are used in the scattering calculations. This last version would be more helpful from the point of application to three-dimensional non-collinear problems. Results obtained by raising the number of elements, or by increasing the polynomial order, are compared. General formulas for the formfunctions in case of arbitrary order of the polynomials will be presented.

Key words: Finite elements – S-matrix reactive scattering

1. Introduction

In the last years considerable progress has been made in the quantum scattering treatment of elementary reactions, using a variety of time-dependent and time-independent approaches [1]. Especially the variational methods have been very successful. The S-matrix version of the Hulthén–Kohn variational principle is one of the general and straightforward approaches which may be applied alternatively

* Dedicated to the 60th birthday of Prof. Jan Linderberg (Aarhus)

to other more standard approaches, especially when applying finite elements (FE) to provide the basis set. In earlier work we have described the finite element method (FEM) for bound state problems and R-matrix type scattering calculations by using different orders of polynomials [2].

In the present work we show how the asymptotic part of the scattering wave-function is described by analytical functions and the interior part of the potential including two channels (e.g. in the collinear case) is described by finite element functions within the concept of the Hulthén–Kohn variational principle (HKVP) of Miller and coworkers [3]. Applications for elastic and inelastic calculations have been described recently [2e]. The S-matrix version of the HKVP has proved to be an extremely powerful approach for carrying out quantum mechanical scattering calculations for molecular reactive, electron–molecule [4a] and molecule–surface [4b, c] collisions. A similar approach using the log-derivative method has been used by Manolopoulos et al. [5]. FEM has also been applied successfully in combination with hyperspherical coordinates for solving 3D reactive scattering and bound state problems [6].

In this paper we show that instead of a product of conventional basis functions for translation and vibration, two-dimensional finite element functions can be employed (no separation ansatz). Two ways of choosing the grid points are used: A) a grid is built that covers both reaction channels and B) we considered the two channels separately and constructed a common overlap.

Within FEM two approaches for the wavefunctions are used: a) in the conventional way finite element functions are taken as basis functions for the interior region and b) first a set of eigenfunctions (using FEM) for the interior region is calculated and then these orthonormal functions are used for calculations at different collision energies. Results obtained by increasing the number of elements or by increasing the polynomial order are compared. General formulas for the formfunctions in case of arbitrary polynomial order will be presented.

The theories of FEM and of the S-matrix version of the Hulthén–Kohn variational principle have already been presented elsewhere [2e, 3a]. So in Sects. 2 and 3 only a short overview will be given. In Sect. 4 we will describe the different shapes for the interaction region that have been choosen. In Sect. 5 the application for the collinear $H + H_2$ reaction will be investigated. Section 6 will end up with the conclusion.

2. The finite element method

The general idea of FEM applied to solve the Schrödinger equation is to change over from the integration to a summation over many subdomains called elements [2a, 6]. On each element the wavefunction is approximated by a parametrized function u. The simplest choice are polynomials of different degrees e.g. in two dimensions (Fig. 1)

$$u(x, y) = \sum_{i,j} c_{ij} x^i y^i. \tag{1}$$

On each element e a certain number of grid points is choosen and the function u on the element is expanded as

$$u^{(e)}(x, y) = \sum_{i=1}^{p} u_i^{(e)} \tilde{N}_i^{(e)}(x, y) = \sum_{i=1}^{p} u_i^{(e)} N_i^{(e)}(\zeta_1, \zeta_2, \zeta_3), \quad u_i^{(e)} = u(x_i, y_i); \tag{2}$$

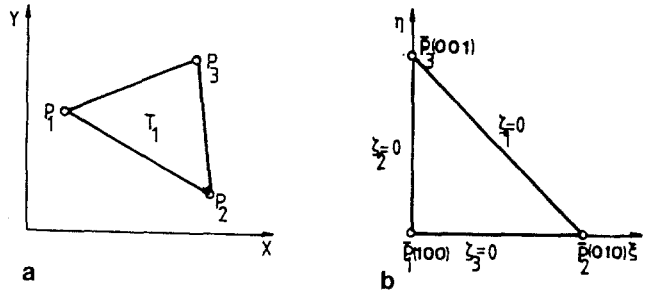

Fig. 1a. General triangle T_1, **b** Natural coordinates in unit triangle with points $\bar{P}_i(\zeta_1, \zeta_2, \zeta_3)$

where the formfunctions $\tilde{N}_i^{(e)}$ ($N_i^{(e)}$) are defined to have interpolating properties inside each element e and are zero or one at the grid points:

$$\tilde{N}_i^{(e)}(x_j, y_j) = \delta_{ij}. \tag{3}$$

Integrals over the whole domain of the problem are then sums over all elements.

We choose a triangular form of the elements (Fig. 1a). One obtains a simple integration formula, if one transforms from an arbitrary triangle to a unit rectangular triangle with the coordinates ξ and η and then to "natural triangular coordinates" ζ_i (Fig. 1a, b):

$$\begin{aligned} x &= x_1 + (x_2 - x_1)\xi + (x_3 - x_1)\eta, \\ y &= y_1 + (y_2 - y_1)\xi + (y_3 - y_1)\eta. \end{aligned} \tag{4}$$

$$\zeta_1 = 1 - \xi - \eta, \quad \zeta_2 = \xi, \quad \zeta_3 = \eta. \tag{5}$$

The formfunctions can then be expressed in terms of the ζ_i. Usually explicit formulas for the formfunctions are used. However, these formulas are given in textbooks only for certain orders of polynomials, for example, second, third and fifth. General formulas in one dimension have been already given in Ref. [2c]. We want to present general formulas for all $(g + 1)(g + 2)/2$ formfunctions of a polynomial of the arbitrary order g in two dimensions.

All the formfunctions are determined by the following three formulas. The formulas depend on the position of the reference points.

If the polynomial order is equal to 3 times a natural number, there exists a point in the center of the triangle (marked by a circle in Fig. 2) with corresponding formfunction

$$N_i = \frac{1}{(n!)^3} \prod_{j=0}^{n-1} (g\zeta_1 - j)(g\zeta_2 - j)(g\zeta_3 - j). \tag{6}$$

Here n is the number of the perimeter on which the point is lying minus 1 (see Fig. 2)

If a point is located in the middle of a side of the triangle itself or of one of the internal perimeters (marked as a cross in Fig. 2), the corresponding formfunction is

$$N_i = \frac{1}{((g/2 - n)!)^2} \prod_{j_1=0}^{g/2-n-1} (g\zeta_1 - j_1)(g\zeta_2 - j_1) \prod_{j_2=0}^{n-1} (g\zeta_3 - j_2). \tag{7}$$

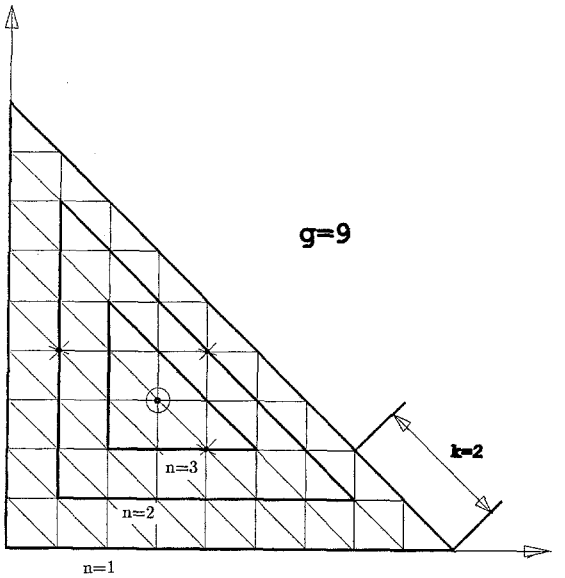

Fig. 2. Grid points in a triangle for a ninth-order polynomial expansion. The outer perimeter defines the triangle ($n = 1$), the central point defines the most internal perimeter ($n = 4$)

For all the other points the formfunctions are:

$$N_i = \frac{1}{(g-2n-k)!(n+k)!n!} \prod_{j_1=0}^{g-2n-k-1} (g\zeta_1 - j_1) \prod_{j_2=0}^{n+k-1} (g\zeta_2 - j_2) \prod_{j_3=0}^{n-1} (g\zeta_3 - j_3). \tag{8}$$

Here k is the distance from the nearest corner (see Fig. 2). ζ_1 is the natural coordinate that is related to this corner, ζ_2 – to the one that is more far from the point, but is lying on the same side.

3. S-matrix version of the Hulthén–Kohn variational principle

In the S-matrix version of the HKVP [7] as derived by Miller and coworkers [3], the S-matrix at energy E is given by

$$S_{n_2,n_1} = ext[c_{1n_2n_1} + \frac{i}{\hbar} \langle \tilde{\Psi}_{n_2} | H - E | \tilde{\Psi}_{n_1} \rangle], \tag{9}$$

where $\tilde{\Psi}_{n_i}(r)$ is a trial wavefunction which is regular at $r = 0$ and has the asymptotic form (for $r \to \infty$)

$$\tilde{\Psi}^E_{n_2}(r, \{q\}) = \sum_n (- u_{0n_i}(r)\delta_{nn_i} + \sum_{l=1}^{N} u_{ln}(r) c_{ln,n_i}) \phi_n(\{q\}). \tag{10}$$

r is the translational coordinate and $\{q\}$ denotes the coordinates of all internal degrees of freedom with the channel eigenfunctions $\{\phi_n(\{q\})\}$. This is the multi-channel formulation for $\tilde{\Psi}(r, \{q\})$ which can be used for elastic (without $\{q\}$ and ϕ_{n_i}), inelastic and reactive processes (with introduction of the indices 1, 2 for the arrangements A + BC and AB + C in the collinear case). The $\{u_{ln}(r)\}$,

$l = 2, \ldots, N$ is a square integrable basis set. $u_{0n}(r)$ and $u_{1n}(r)$ have the properties of incoming and outgoing waves, which can be "free" functions (the special form depends on the dimension of space to be included) or distorted functions. In order to regularize u_{0n} and $u_{1n}(u_{1n} = u_{0n}^*)$, they are multiplied by a cutoff function. We have choosen

$$u_{0n} = f(r)\mathrm{e}^{-ik_n r} v_n^{-1/2}, \quad v_n = \frac{\hbar k_n}{\mu}, \quad k_n = \left(\frac{2\mu(E - E_n)}{\hbar^2}\right)^{1/2} \tag{11}$$

and

$$f(r) = \tfrac{1}{2}\{1 + \tanh[\alpha(r - r_\alpha)]\}. \tag{12}$$

Stationarity of Eq. (9) with respect to the expansion coefficients c_{ln_i,n_j} (in Eq. 10) leads to the matrix equation (details see [3a])

$$\boldsymbol{S} = \frac{\boldsymbol{i}}{\hbar}(\boldsymbol{B} - \boldsymbol{C}^T \boldsymbol{B}^{*-1} \boldsymbol{C}), \tag{13}$$

where $\boldsymbol{S}, \boldsymbol{B}$ and $\boldsymbol{C}$ are matrices of the size of the number of open channels. $\boldsymbol{B}$ and $\boldsymbol{C}$ are given by

$$\boldsymbol{B} = \boldsymbol{M}_{00} - \boldsymbol{M}_0^{\mathrm{T}} \boldsymbol{M}^{-1} \boldsymbol{M}_0, \tag{14}$$

$$\boldsymbol{C} = \boldsymbol{M}_{10} - \boldsymbol{M}_0^{*\mathrm{T}} \boldsymbol{M}^{-1} \boldsymbol{M}_0, \tag{15}$$

$$(M_{00})_{nn'} = \langle u_{0n}\phi_n | H - E | u_{0n'}\phi_{n'} \rangle, \tag{16}$$

$$(M_{10})_{nn'} = \langle u_{1n}\phi_n | H - E | u_{0n'}\phi_{n'} \rangle, \tag{17}$$

$$(M)_{ln,l'n'} = \langle u_l\phi_n | H - E | u_{l'}\phi_{n'} \rangle, \quad l, l' = 2, \ldots, N, \tag{18}$$

$$(M_0)_{ln,n'} = \langle u_l\phi_n | H - E | u_{0n'}\phi_{n'} \rangle, \quad l = 2, \ldots, N. \tag{19}$$

The translational functions in the bra symbols in Eqs. (16) and (17) are not the complex conjugate ones, and n is the collective index of all internal quantum numbers.

The main numerical effort in this scattering method is the calculation of matrix elements. Those in Eqs. (16), (17) and (19) have to be recalculated for each energy. The matrix elements of the Hamiltonian and the overlap matrix over the basis $u_l\phi_n$, $l \geqslant 2$, in Eq. (17) have to be calculated only once, but the inversion of $\boldsymbol{M}$ has to be repeated for each energy. In order to reduce the size of the matrices in Eqs. (14 and 15), different polynomial orders for finite elements and different potential adapted basis sets have been tested.

In the case of solving the scattering problem the wavefunction is built up from FE-functions in the interior region and analytical functions in the asymptotic region.

However in the case of applying the original FE-functions much computing time has to be spent for "inverting" the large matrix (Eqs. (14) and (15)). Alternatively we first solve the eigenvalue problem within FEM

$$(\Psi^{\mathrm{FEM}} | H | \Psi^{\mathrm{FEM}}) = E'(\Psi^{\mathrm{FEM}} | \Psi^{\mathrm{FEM}}) \tag{20}$$

up to a maximum eigenvalue $E_{\max}$ or up to a finite number of eigenfunctions, which are then used as a new orthogonal basis for calculating the matrix elements in

Eqs. (18) and (19). The inversion of the large matrix $\boldsymbol{M}$ for different energies is then just the inversion of the diagonal elements.

4. Grid schemes for calculating a potential adapted basis

In order to reduce the amount of computing time (that is related to solving the linear equation in Eq. (14)) we tried to find out if eigenfunctions that cover different reaction channels can be choosen to build up a more effective basis set. This would be even more interesting for polyatomic systems if for each channel, potential adapted eigenfunctions (in more than one dimension) can be made available. The problem that one has to deal with is the linear dependency. In the present case it could be easily handled by choosing those basis functions that have eigenvalues of the complete overlap matrix larger than say $\varepsilon \approx 10^{-1}$ a.u. In Fig. 3a–d the different shapes for the finite element regions (used in the calculations) are shown. Fig. 3a shows an area that includes the incoming and the outgoing arrangement channel. In Fig. 3b, c shapes are presented for the potential areas where only one channel each is included; by increasing the size of the shapes the overlap increases. Fig. 3d includes the complete area for the whole reaction including the break up into the three atoms. This latter form is only useful when the elements are chosen appropriately.

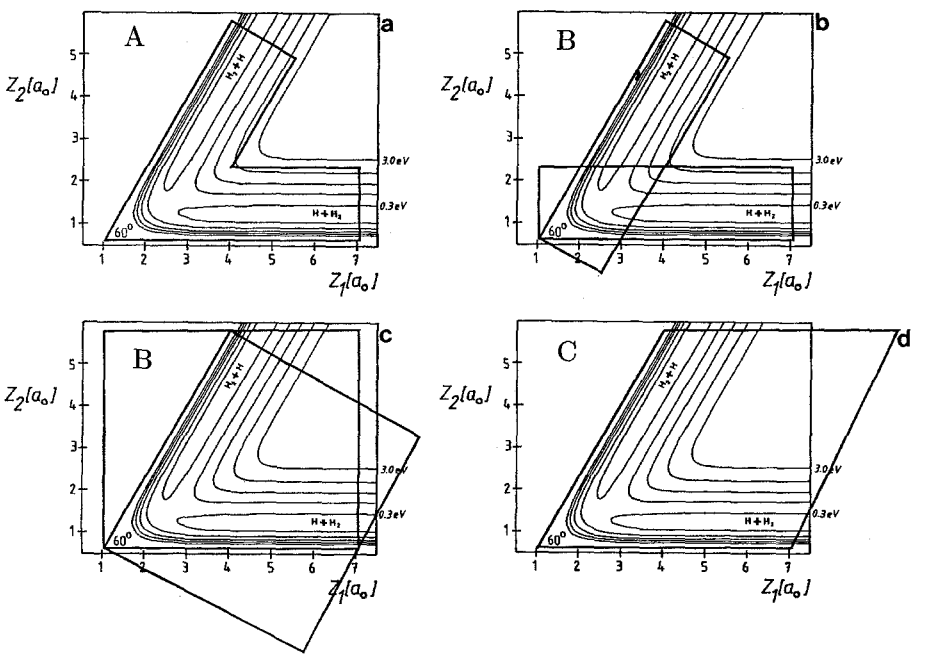

Fig. 3. Porter–Karplus-potential [8] in mass-weighted coordinates Z_1, Z_2 for the collinear reaction H + H_2[3a]. Different grid schemes for calculating a potential adapted adiabatic basis from finite element functions: **a** v-shaped region A (including two arrangement channels), **b** and **c** two rectangular shapes B (depending on the size: two independent arrangement channels or two arrangement channels included in one grid scheme), **d** rhomboedrical shape C (including both arrangement channels)

5.1. Application to collinear reaction

The discussion in the Sects. 5a and b is related to the problem how sensitive the results are with respect to the total size and form of the finite element region and the different orders of the polynomial expansion. A detailed comparison of different scattering methods using conventional basis set approaches has already been given in Ref. [2a] for the collinear H + H_2-reaction using the R-matrix method with finite elements. A comparison of the S-matrix HKVP-approach using FE in comparison with basis sets was discussed in Ref. [2e] for the inelastic (2D) He + H_2-collision.

In Table 1 results of the reaction probabilities $P^{re}_{v,v'}$ for the collinear $H + H_2(v) \rightarrow H_2(v') + H$ reaction (Porter–Karplus potential [8]) using different versions with original finite elements (FE) and FE-eigenfunctions (FE-EF) for different shapes (Fig. 3: A, B, C) of the interaction region and different energies are shown. For comparison some earlier work of Rosenthal and Gordon [9] and Diestler [10], using finite differences, is quoted.

For energy $E_{tot} = 0.8426$ eV detailed informations about the shape sizes and forms are given. For shape A and with the original FE-functions roughly 61–81 grid points in x direction (translation) and 31–41 grid points in y direction (vibration) are needed in order to reach an accuracy of better than 1% (see No. 5, 6 in Table 1). By choosing 70 FE-EF ($N_x = 61$, $N_y = 31$) the accuracy is fairly good, but with 100 FE-EF we reached nearly the accuracy of the original FE calculations. Increasing the number of eigenfunctions from 100 to 150 does not change the results very much (No. 11–13). If one increases the size of the shape ($x = 8 \rightarrow 12$, $y = 4 \rightarrow 6$) the number of choosen FE-EF has to be increased in case the number of grid points is kept the same (No. 14–16). But even more accurate results can be achieved, when increasing the number of grid points and using 100–150 eigenfunctions (No. 14–19). The eigenfunctions have to be calculated only once and can be used for all scattering energies $E_{tot} < 0.8426$ eV and at least for energies 20% larger. The additional computing amount for different scattering energies $E_{tot} < \approx 1.0$ eV is negligible.

Using shape B again roughly 100 eigenfunctions are enough to calculate the reaction probability accurately (No. 28, $x = 8$, $y = 8$), but in case that the overlap of the different arrangement channel FE-EF is not good enough (see Fig. 3b, in vibrational direction the shape is not broad enough) no correct reaction probability is obtained (No. 20–22). That the calculations for the shape B ($x = 8$, $y = 4$) do not lead to correct results is not easy to understand. There might be a problem with the buildup of the linear independent basis set in the interior region or with the coupling of the asymptotic wavefunction for one arrangement channel with the interior basis set of the other arrangement channel. Another possibility is that most of the eigenfunctions calculated for separate arrangement channels are not useful for the coupling between the two arrangement channels to give a correct physical picture as by using shape A or C.

Shape C covers the complete interaction area (including complete breakup), so that at least $N_x = 61$ grid points have to be choosen in the y direction (No. 29–32).

If one increases the scattering energy the size of shape A has to be increased in order to describe the wavefunction correctly until it reaches the size of shape C. The number of grid points has not to be increased very much (see Table 1, No. 6, 37, 40). The number of FE-EF has to be enlarged (one should choose for $E_{max} \approx 2E_{tot}$ (E_{max} is the cutoff for the eigenfunctions included), but as said before, all eigenfunctions can be used for all scattering energies $E_{tot} < E_{max}/2$.

Table 1. Reaction probabilities $P^{re}_{v,v'}$ for collinear $H + H_2(v) \rightarrow H_2(v') + H$ using different methods with original finite elements (FE) and FE-eigenfunctions (FE-EF). S-matrix FEM calculations with 5th-order FE-functions. For explanation of the different shapes see Fig. 3. Values in parentheses are the powers of ten[a]

Method	E_{tot}(eV)	P^{re}_{00}	P^{re}_{01}	P^{re}_{11}	P^{re}_{02}	P^{re}_{12}	P^{re}_{22}	N^b_x	N^b_y	x^b	y^b	Comments	No.
R-matrix FEM [2a]	0.8426[c]	0.852	0.303(−2)	0.200(−3)									1
Rosenthal and Gordon [9]		0.858	0.238(−2)	0.15(−3)									2
Diestler (FD) [10]		0.853	0.3(−2)	0.2(−3)									3
S-matrix FEM		0.864	0.317(−2)	0.224(−3)				41	21	8	4	Orig. FE, shape A	4
		0.855	0.324(−2)	0.238(−3)				61	31	8	4	Orig. FE, shape A	5
		0.854	0.324(−2)	0.238(−3)				81	41	8	4	Orig. FE, shape A	6
		0.907	0.227(−2)	0.152(−2)				41	21	8	4	50 FE-EF, shape A	7
		0.851	0.317(−2)	0.290(−3)				61	31	8	4	70 FE-EF, shape A	8
		0.855	0.346(−2)	0.232(−3)				61	31	8	4	100 FE-EF, shape A	9
		0.856	0.346(−2)	0.260(−3)				81	41	8	4	100 FE-EF, shape A	10
		0.855	0.346(−2)	0.231(−3)				61	31	8	4	100 FE-EF, shape A	11
		0.854	0.345(−2)	0.232(−3)				61	31	8	4	120 FE-EF, shape A	12
		0.854	0.345(−2)	0.233(−3)				61	31	8	4	150 FE-EF, shape A	13
		0.864	0.302(−2)	0.227(−3)				81	41	12	6	100 FE-EF, shape A	14
		0.854	0.321(−2)	0.270(−3)				81	41	12	6	120 FE-EF, shape A	15
		0.854	0.316(−2)	0.240(−3)				81	41	12	6	150 FE-EF, shape A	16
		0.855	0.326(−2)	0.240(−3)				101	51	8	4	100 FE-EF, shape A	17
		0.854	0.324(−2)	0.238(−3)				101	51	8	4	150 FE-EF, shape A	18
		0.853	0.314(−2)	0.248(−3)				101	51	12	6	150 FE-EF, shape A	19
		0.965	0.515(−1)	0.136				61	61	8	4	100 FE-EF, shape B	20
		0.834	0.559(−1)	0.196				71	71	8	4	100 FE-EF, shape B	21
		0.759	0.515(−1)	0.220				81	81	8	4	100 FE-EF, shape B	22
		0.885	0.173(−2)	0.211(−2)				61	61	8	6	100 FE-EF, shape B	23
		0.851	0.476(−2)	0.234(−3)				71	71	8	6	100 FE-EF, shape B	24
		0.852	0.344(−2)	0.186(−3)				81	81	8	6	100 FE-EF, shape B	25

		0.772	0.199(−1)	0.837(−2)				61	61	8	8	100 FE-EF, shape B	26
		0.833	0.936(−2)	0.883(−3)				71	71	8	8	100 FE-EF, shape B	27
		0.857	0.334(−2)	0.246(−3)				81	81	8	8	100 FE-EF, shape B	28
		0.859	0.264(−2)	0.230(−3)				61	61	8	8	150 FE-EF, shape C	29
		0.860	0.266(−2)	0.236(−3)				61	61	8	8	100 FE-EF, shape C	30
		0.855	0.315(−2)	0.218(−3)				71	71	8	8	100 FE-EF, shape C	31
		0.855	0.324(−2)	0.237(−3)				81	81	8	8	100 FE-EF, shape C	32
R-matrix FEM [2a]	1.2966	0.562	0.110	0.150	0.3(−3)	0.22(−3)	< 0.1(−4)						33
Rosenthal and Gordon [9]		0.663	0.070	0.214	0.95(−4)	0.47(−4)	0.32(−7)						34
S-matrix FEM		0.571	0.108	0.151	0.289(−3)	0.329(−3)	0.562(−6)	61	31	8	4	Orig. FE, shape A	35
		0.569	0.107	0.149	0.222(−3)	0.325(−3)	0.509(−6)	61	31	10	5	Orig. FE, shape A	36
		0.567	0.107	0.151	0.295(−3)	0.331(−3)	0.576(−6)	81	41	8	4	Orig. FE, shape A	37
R-matrix FEM [2a]	1.4466	0.135	0.216	0.225	0.100	0.138	0.530						38
Rosenthal and Gordon [9]		0.153	0.233	0.198	0.086	0.120	0.530						39
S-matrix FEM		0.133	0.216	0.227	0.100	0.138	0.522	81	41	10	5	Orig. FE, shape A	40

[a] Parameters for the cutoff function (Eq. (12)): $\alpha = 2a_0^{-1}, r_\alpha = 5.5a_0$

[b] Shape A: N_x, N_y: number of points per arrangement channel, x, y: size of one arrangement channel (non-mass-weighted, different to picture in Fig. 3) Shape B, C: N_x, N_y: total number of points in x, y direction, x, y: total size (non-mass-weighted)

[c] Converged results for $E_{tot} = 0.8426$ eV see No. 3 in Table 2

5.2. *Use of higher-order polynomials*

The collinear model system $H + H_2$ has also been used for testing polynomials of different orders for the finite elements. According to the results summarized in Table 2, the use of higher-order polynomials leads to a reduction of the number of grid points needed (No. 1–3). One has to keep in mind that in all calculations an equidistant grid was used and that in case of an optimized grid even less points would be needed. In case of No. 2 there are only three elements used for the vibrational direction.

In case of the size $x = 8$, $y = 4$ (No. 3–6) increasing the polynomial order from 5 to 8 does not change the results, with 5th order they are already converged. If one increases the size of shape A (No. 7–9) 7th and 8th order polynomials are flexible enough to calculate correct values as for a smaller shape (No. 3, 6).

The use of 80 FE-EF calculated with different orders (No. 10–14) leads to nearly correct results, if at least $N_x \approx 61$ and $N_y \approx 31$ points are used. Increasing the size of the shape one needs in addition a larger number of FE-EF, but if in addition the N_x, N_y points are not increased to (81, 41) or (101, 51) the results will be less good (No. 15–19).

In case of the original FE there was enough flexibility by keeping 8th order and increasing the shape (No. 3, 9), but in case of eigenfunctions this does not help (No. 18, 19). This can be interpreted in the way that with original FE the use of even higher-order polynomials than 5 is numerically effective, but in case of applying potential adapted basis functions one can use 5th-order polynomials and with more grid points, if needed.

However, the matrix structure of the hamiltonian matrix becomes less sparse when using higher-order polynomials. This influences the time of solving the eigenvalue problem. So it depends on the numerical eigenvalue solver and the architecture of the computer which way is more effective, i.e. less grid points and higher order or more grid points and lower order.

6. Conclusion

We have shown that instead of conventional L^2-basis functions FE-functions (that cover different sizes of the potential region) can be used efficiently for calculating the S-matrix via the Hulthén–Kohn variational principle. Finite elements have the advantage that they can be optimally adapted to different areas of the interaction region [2c]. One has the flexibility of choosing different orders of the polynomials and different shapes for each element. FEM allows to obtain realistic estimates of the accuracy and convergence properties. In the future we are going to use a multigrid technique which has the advantage of automatic optimization of grid points and an increased efficiency of solving linear equations and eigenvalue problems [11]. The idea in this paper of testing different shapes for the interaction region is to build up a modular basis set of functions for different arrangement channels that might be useful for exact 3D reactive A + BC-scattering calculations or for even larger polyatomic systems where one is interested in special arrangement problems. The presented way of performing the scattering calculations is in the mode of extension to three-dimensional scattering, where the full 3D eigenfunctions of the ABC-molecule (for bound and unbound ABC-systems) are taken into account. Preliminary calculations using finite element techniques for calculating e.g. the

Table 2. S-matrix FEM calculations for the reaction probabilities $P^{re}_{v,v'}$ for collinear $H + H_2(v) \rightarrow H_2(v') + H$ using polynomials of different orders with original finite elements (FE) and FE-eigenfunctions (FE-EF). $E_{tot} = 0.8426$ eV. Explanations see Table 1

P^{re}_{00}	P^{re}_{01}	P^{re}_{11}	Order	N_x	N_y	x	y	Comments	No.
0.884	0.363(−2)	0.836(−4)	8	33	17	8	4	Orig. FE, shape A	1
0.856	0.322(−2)	0.237(−3)	8	49	25	8	4	Orig. FE, shape A	2
0.854	0.324(−2)	0.238(−3)	8	65	33	8	4	Orig. FE, shape A	3
0.855	0.324(−2)	0.238(−3)	5	61	31	8	4	Orig. FE, shape A	4
0.854	0.324(−2)	0.238(−3)	6	61	31	8	4	Orig. FE, shape A	5
0.855	0.324(−2)	0.238(−3)	7	57	29	8	4	Orig. FE, shape A	6
0.854	0.323(−2)	0.237(−3)	7	57	29	10	5	Orig. FE, shape A	7
0.854	0.324(−2)	0.238(−3)	8	65	33	10	5	Orig. FE, shape A	8
0.853	0.324(−2)	0.237(−3)	8	65	33	12	6	Orig. FE, shape A	9
0.858	0.317(−2)	0.237(−3)	4	65	33	8	4	80 FE-EF, shape A	10
0.858	0.342(−2)	0.229(−3)	5	61	31	8	4	80 FE-EF, shape A	11
0.865	0.327(−2)	0.246(−3)	6	61	31	8	4	80 FE-EF, shape A	12
0.960	0.146(−1)	0.277(−3)	7	29	15	8	4	80 FE-EF, shape A	13
0.865	0.313(−2)	0.246(−2)	7	57	29	8	4	80 FE-EF, shape A	14
0.855	0.274(−2)	0.232(−3)	5	61	31	10	5	100 FE-EF, shape A	15
0.857	0.338(−2)	0.185(−3)	5	61	31	12	6	100 FE-EF, shape A	16
0.864	0.300(−2)	0.235(−3)	5	101	51	12	6	100 FE-EF, shape A	17
0.872	0.302(−2)	0.219(−3)	8	65	33	12	6	100 FE-EF, shape A	18
0.865	0.320(−2)	0.225(−3)	8	65	33	12	6	150 FE-EF, shape A	19

bound states of H_3^+ have already been tested [12], so that an extension to scattering can be achieved relatively easy.

Acknowledgements. The authors thank V. Staemmler, W. H. E. Schwarz and A. Kumpf for discussions. R. J. thanks the HLRZ-Jülich for supplying computer time on the Cray-YMP.

References

1. a. Miller WH (1990) Ann Rev Phys Chem 41:245 and references therein
   b. Truhlar DG, Sckwenke DW, Kouri DJ (1990) J Phys Chem 94:7346 and references therein
   c. Baram A, Last I, Baer M (1993) Chem Phys Lett 212:649
   d. Kupperman A, Wu Y-SM (1993) Chem Phys Lett 205:577
   e. Launay JM, LeDeurneuf M (1990) Chem Phys Lett 169:473
   f. Neuhauser D, Judson D, Jaffe R, Baer M, Kouri DJ (1991) Chem Phys Lett 176:546
   g. Chatfield DC, Reeves MS, Truhlar DG, Duneczky C, Schwenke DW (1992) J Chem Phys 97:8322
   h. Marković N, Billing GD (1992) J Chem Phys 97:8201
2. a. Jaquet R (1987) Theoret Chim Acta 71:425
   b. Jaquet R (1989) In: Lagana A (ed), Supercomputer algorithms for reactivity, dynamics and kinetics of small molecules. Kluwer, Dordrecht
   c. Jaquet R (1990) Comp Phys Comm 58:257
   d. Jaquet R (1992) Habilitationsschrift (1987), Siegen. Shaker. Aachen
   e. Jaquet R, Schnupf U (1992) Chem Phys 165:287
   f. Schnupf U (1990) Diplom thesis. Siegen. Germany
3. a. Zhang JZH, Chu SI, Miller WH (1988) J Chem Phys 88:6233
   b. Miller WH (1988) Comments At Mol Phys 22:115
   c. Zhang JZH, Miller WH (1987) Chem Phys Lett 140:329
   d. Zhang JZH (1991) J Chem Phys 94:6047
   e. Colbert DT, Miller WH (1992) J Chem Phys 96:1982
   f. Belyaev AK, Colbert DT, Groenenboom GC, Miller WH (1993) Chem Phys Lett 209:309
4. a. Rescigno TN, McCurdy CW, Schneider BI (1989) Phys Rev Lett 63:248
   b. Sheng J, Zhang JZH (1992) J Chem Phys 97:6784 (1993) J Chem Phys 99:1373
   c. Saalfrank P, Miller WH (1993) J Chem Phys 98:9040
5. Manolopoulos D, D'Mello M, Wyatt RE (1990) J Chem Phys 93:403
6. a. Linderberg J (1986) Int J Quant Chem Symp 19:467
   b. Linderberg J, Padkjaer SB, Öhrn Y, Vessal V (1989) J Chem Phys 90:6254
   c. Pack RT, Parker GA (1987) J Chem Phys 87:3888
   d. Kuppermann A, Hipes PG (1986) J Chem Phys 84:5962
   e. Soarez Neto JJ, Padkjaer SB, Linderberg J (1989) Int J Quant Chem 23:127
   f. Linderberg J (1992) Int J Quant Chem Symp 26:717
7. a. Hulthén L (1994) Kgl Fysiogr Sallsk Lund Förh 14:21
   b. Hulthén L (1948) Arkiv Mat Astron Fysik 35A:25
   c. Kohn W (1948) Phys Rev 74:1763
   d. Nesbet RK (1980) Variational methods in electron atom scattering theory. Plenum, New York
   e. Joachain CJ (1983) Quantum collision theory. Elsevier, Amsterdam
8. Porter RN, Karplus M (1964) J Chem Phys 40:1105
9. Rosenthal A, Gordon RG (1976) J Chem Phys 64:1641
10. Diestler DJ (1971) J Chem Phys 54:4547
11. Hackbusch W (1985) Multigrid methods and applications. Springer, Heidelberg
12. Jaquet R, unpublished